

Laser action in strongly scattering rare-earth-metal-doped dielectric nanophosphors

G. R. Williams, S. B. Bayram, and S. C. Rand

Division of Applied Physics, Randall Laboratory, University of Michigan, Ann Arbor, Michigan 48109-1022

T. Hinklin and R. M. Laine

Department of Materials Science & Engineering, University of Michigan, Ann Arbor, Michigan 48109

(Received 24 October 2000; revised manuscript received 5 June 2001; published 11 December 2001)

We report continuous-wave laser action in two oxide nanopowders doped with Ce^{3+} and Pr^{3+} ions. To our knowledge, these are the first observations of stimulated emission from electrically pumped random media in which scattering and distributed feedback scale lengths are much shorter than a wavelength. The continuous nature of the laser emission in small volumes (on the order of a cubic wavelength) of these low gain systems, and the absence of coherent speckle, provide compelling evidence that these results are mediated by strong Anderson localization of light.

DOI: 10.1103/PhysRevA.65.013807

PACS number(s): 42.55.Rz, 42.25.Fx

I. INTRODUCTION

Previous experiments [1–9] and theory [10,11] on localization of light and stimulated emission [12–16] in scattering media, as well as questions regarding the consequences of recurrent scattering events [17,18], have all heightened current interest in electromagnetic phenomena in multiply scattering media. Surprisingly few theoretical or experimental papers have been published, however, that relate to the limiting regime in which mean free paths and interparticle spacings are much less than a wavelength. Traditionally, multiple scattering has been of interest to researchers studying statistical aspects of weakly localized light [19], coherence [20], or imaging [21]. Others have utilized multiple scattering to achieve pulsed laser action in powders where electromagnetic propagation is diffusive [2,5,8]. However, at the boundary between the diffusive and strong scattering regimes where transport distances are on the order of the wavelength, fundamental changes are anticipated in the interaction of light with matter that are new and unstudied. In particular, severe scattering is predicted to cause strong localization of light in lossless systems, over limited frequency ranges [10,11], although such behavior is not evidenced in mean-field calculations [22].

Confinement of light by lossless scattering within three-dimensional (3D) regions of subwavelength dimensions, if it were to occur in *dense random* media, would have profound effects on coherence and light-scattering properties of the medium since “propagation” would then be restricted to distances less than an oscillation period ($l^* < \lambda$). For unabsorbed waves to be localized to the extent that they do not propagate even one wavelength in any direction, dramatic changes in propagation parameters have to take place that are not predicted by effective-medium theory. For instance, in order for an electromagnetic disturbance to cease oscillating spatially in a nonabsorbing medium, the local wave vector must lose its directional character and definition as a real quantity altogether. Consequently, computations of coherent superpositions of multiply scattered fields are needed, without the averaging that is customarily performed over one or more wavelengths to define constitutive parameters, to inves-

tigate optical properties in this regime theoretically. Some specific predictions have already been made, however, and thresholds for laser action mediated purely by scattering are expected to drop dramatically under strong scattering conditions [13,16].

Here we report for the first time, to our knowledge, results related to this latter prediction, by demonstrating continuous-wave, electrically pumped powder lasers. We have generated ultraviolet and visible laser radiation in dry, rare-earth-doped nanopowders excited by a continuous, low-voltage, and low-current electron beam. Earlier publications on pulsed laser action in powders were optically pumped experiments in rare-earth [2,5,8] and polymeric [23] materials in the diffusive regime and in semiconductor powders [24,25], where angular dependences in output spectra and modes were reported [23–25]. The angular variations in previous results indicated that different microcavities were responsible for output in different directions. The observation of frequency selectivity within the transition bandwidth (modes) also provided clear spectroscopic evidence that the effective lengths of the laser cavities were much greater than half a wavelength. In Refs. [23–25], the effective cavity lengths deducible from output spectra exceeded ten wavelengths (see *Note added in proof*). Since spectral and angular variations reflect nonrandom aspects of material properties and propagation on length scales greater than an optical wavelength, these observations in earlier pulsed powder lasers showed that the scattering paths responsible for lasing, while short, were still too long to randomize laser output completely. It may be readily appreciated, however, that if closed paths providing feedback for lasing are shorter than half a wavelength, the constructive and destructive interference of light required to produce frequency selectivity cannot occur. Therefore, for effective source volumes smaller than a cubic half-wavelength, the stimulated-emission spectrum should be quite different from that of a single-mode coherent laser source, occupying the full gain bandwidth and being independent of viewing angle. In the phosphors described here, we have observed unusual features of this kind, in the presence of conventional indicators of laser action such as sharp thresholds, linear output,

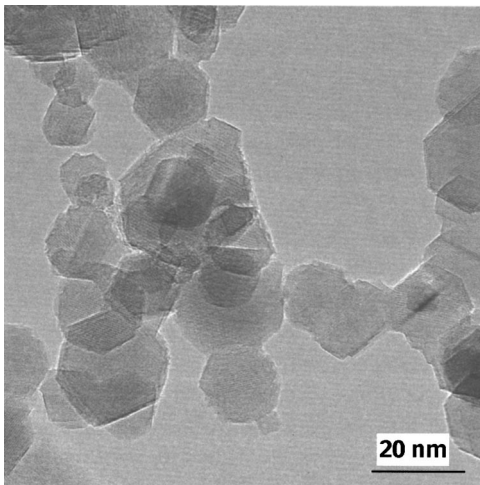


FIG. 1. Transmission electron micrograph of δ - Al_2O_3 nanoparticles. Note the faceted edges, and the unaggregated state, of particles in the sample.

and spectral quenching of competing transitions from the upper state.

II. EXPERIMENT

Our samples consisted of δ -alumina nanopowders synthesized by flame spray pyrolysis and doped with the rare-earth-metal ions Ce^{3+} and Pr^{3+} at concentrations of 1000 ± 100 ppm [26]. Metallo-organic precursors consisting of alumatrane $[\text{N}(\text{CH}_2\text{CH}_2\text{O})_3\text{Al}]$ with an equivalent loading of 2 wt. % Al_2O_3 , and nitrate equivalents of 0.003 wt. % CeO_2 or PrO_2 dissolved in ethanol were used to produce powders by combustion at ~ 2000 °C in oxygen at rates over 50 g/h. Particles were collected electrostatically downstream from the flame. Particle sizes were estimated using BET [27] surface areas (80 ± 1 and 43 ± 1 m^2/g for Ce and Pr) and x-ray line broadening. The unaggregated, single-crystal nature of the particles was confirmed by transmission electron microscopy (Fig. 1).

Dopant concentrations achieved in alumina were estimated to be 75 ions per 20-nm particle in the case of Ce and 800 ions per 40-nm particle for Pr. As-produced powders were excited by a low-current beam from a Kimball-Physics EG-14B electron gun to record optical-emission spectra. Loose powder samples were lightly pressed into (3 mm) shallow recesses of an oxygen-free copper mount in ultra-high vacuum ($< 6 \times 10^{-10}$ T) and irradiated with electrons in the energy range 1–10 keV over spot diameters of ~ 2 mm. Luminescence was collected with $f/4$ fused silica optics and analyzed with a 1-m grating spectrometer.

Scattering conditions in the powder samples were evaluated using three separate coherent backscattering setups designed to measure $I^*(\lambda)$, the mean distance traveled by light prior to directional randomization [1,28,29]. In the principal method, probe light from an Ar^+ laser (363.8 nm) overlapping the Ce^{3+} emission was used to record backscattered intensity through an interference filter using a 1P28 photomultiplier, while the sample was rotated through an angular

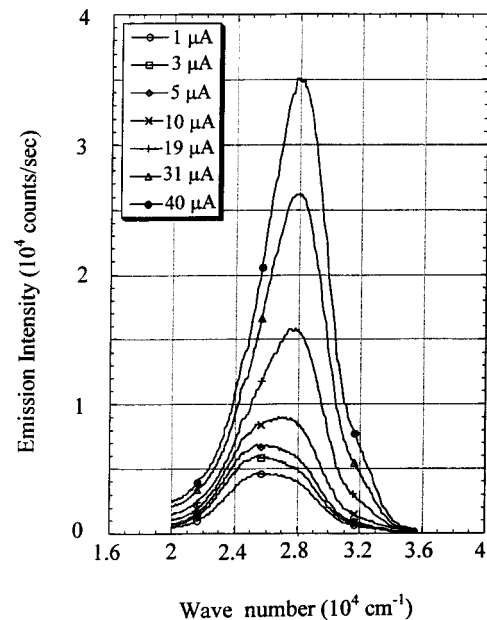


FIG. 2. Cathodoluminescence spectra of Ce: δ - Al_2O_3 nanoparticles excited by various electron-beam current levels (4 keV, 2-mm beam diameter).

range of ± 300 mrad with a step size (2.8 mrad) that exceeded the detection angle (1 mrad). Scattering was recorded for light polarized linearly in the scan plane and perpendicular to it and, in additional runs, for circularly polarized incident light. The photomultiplier was preceded by lensless polarizer and waveplate combinations that detected only polarization-preserving signals. In two other approaches, which yielded similar results, the detector moved in the scanning plane on a mechanical arm of fixed radius (1 m) centered on the sample surface. In one case the incident laser beam was directed to the scattering surface by a micromirror, and in the other by a beamsplitter oriented at 45° to permit intensity measurements over the limited but important backscattering angular range from -10 to $+10$ mrad. In this way many coherent backscattering (CBS) experiments were performed to investigate transport conditions at the wavelengths of importance here.

III. RESULTS

The ultraviolet emission spectrum of Ce^{3+} : δ - Al_2O_3 (Fig. 2) consisted of a partly resolved doublet due to $5d$ - $4f$ inter-configurational transitions of Ce^{3+} [30] and did not vary with observation direction. The separation of the two components of this feature (near $25\,500$ and $28\,000$ cm^{-1}) was consistent with the ${}^2F_{7/2}$ - ${}^2F_{5/2}$ interval (~ 2100 cm^{-1}) of the spin-orbit-split $4f$ ground term of Ce^{3+} in crystals [31,32]. However, the low-energy component disappeared once the current was increased above 12 μA . This phenomenon is known as spectral quenching, and here signals the onset of stimulated emission on the $5d$ - $4f$ (${}^2F_{5/2}$) transition. This is due to the fact that both components of the $5d$ - $4f$ (${}^2F_{5/2}$, ${}^2F_{7/2}$) doublet originate from the *same upper state*. Quenching of one but not the other emissive transition from a single occupied state

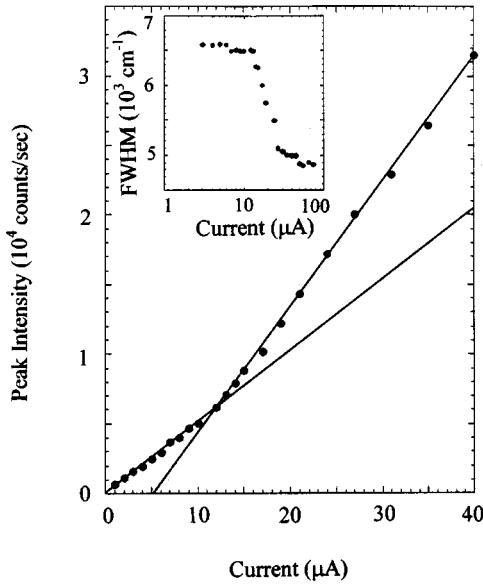


FIG. 3. Peak emission intensity at $\lambda_{em}=362$ nm vs current. Solid curves are guides to the eye. Inset: total linewidth (FWHM) of the composite, ultraviolet emission feature from Ce: δ - Al_2O_3 nanoparticles plotted vs current.

is uniquely attributable to stimulated emission, since this is the only process that can alter the *relative* radiative decay rates of the two $5d$ - $4f$ transitions. This result is remarkable in our experiments because it is obtained with weak *continuous* excitation. The apparent shift of the high-energy component in Fig. 2 to shorter wavelengths as current increased was also consistent with the development of gain on the $5d$ - $4f$ ($^2F_{5/2}$) transition, since increasing gain can progressively offset losses from resonant reabsorption.

In Fig. 3, the intensity of Ce^{3+} emission is plotted versus electron current. The sharp break in slope evident at ~ 12 μA between two *linear* output regimes, and the abrupt spectral quenching of one of the $5d$ - $4f$ components which sets in at the same current (inset), are jointly indicative of stimulated emission with feedback, or laser action. An important distinction may be made between this behavior and that expected for amplified spontaneous-emission processes (ASE) in which the output depends exponentially on the pumping rate [14,33]. Since our small particle sizes preclude optical feedback from high- Q morphological resonances either between near-neighbor particles or within powder grains, a distributed feedback mechanism is necessary to account for these characteristics [34].

Results of coherent backscattering experiments performed to determine average distances over which light is transported in our samples are shown in Fig. 4. The upper curve corresponds to data recorded for Ce^{3+} -doped nano-alumina at 363.8 nm. For Pr-doped samples, a He-Ne laser (632.8 nm) was used, and results obtained with the same approach are given in the lower curve. The inset provides a magnified view of the cusp obtained using the complementary technique described in the preceding section, in which the detector is scanned through an angular range of 20 mrad, collecting light through a beamsplitter. The sharpness of the CBS cusp in all scans sets a lower limit on the absorption length

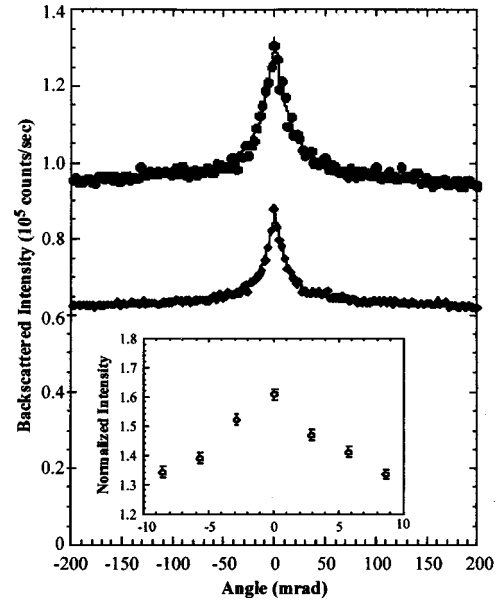


FIG. 4. Experimental backscattered intensity vs angle at $\lambda_{ex} = 363.8$ nm (upper trace) and $\lambda_{ex} = 632.8$ nm (lower trace), from Ce: δ - Al_2O_3 and Pr: δ - Al_2O_3 nanoparticles, respectively (incident polarization perpendicular to scan plane). Solid curves are best fits (see Ref. [4]). Inset: sharp, triangular cusp at exact backscattering in Pr: δ - Al_2O_3 , showing normalized peak intensity of 1.61 after corrections for beamsplitter reflectivity.

of $l_\alpha > 1$ cm for line-shape analysis [35,36]. Least-squares fits [4] to the data then yielded $l^* = 114 \pm 15$ nm at 363.8 nm, and $l^* = 311 \pm 17$ nm at 632.8 nm, the latter value being consistent with the independent determination from slope analysis of the inset data. This analysis requires that the angle-averaged internal reflectivity R of the samples be known at 363.8 and 632.8 nm. Accordingly, R was calculated using dispersion data of pure alumina [37] and found to be $R = 0.711$ and 0.704 , respectively, with no adjustable parameters [4]. Experimentally, mean free transport distances were therefore found to be less than half a wavelength in both instances. These short values nevertheless allow for gain-length products for both ions ($N\sigma_{se}l^* \approx 0.003$ and $N\sigma_{se}l^* \approx 0.0008$ for saturated Ce^{3+} and Pr^{3+} systems, respectively) that substantially exceed the estimated losses ($\gamma l^* = l_\alpha^{-1} l^* < 10^{-5}$).

IV. DISCUSSION

In Sec. III, transport distances (l^*) shorter than half a wavelength were deduced in conjunction with interparticle spacings of less than $\lambda/15$ at both the experimental wavelengths (363.8 and 632.8 nm). The presence of many particles spaced by less than a wavelength on average violates the assumptions of Mie theory, even when extended to multiply scattering media [38], as well as earlier CBS theories [4]. Like previous authors [17], we nevertheless assumed the shape of the backscattering cone and its relation to the transport distance l^* were unchanged under strong scattering conditions. The maximum height of the cone with respect to the incoherent background is known to decrease in the strong

scattering regime [17], so it may not be too surprising that the contrast in our CBS scans is substantially lower than 2, even in the helicity-preserving channel. However, the short l^* values obtained from analyzing light polarized perpendicular to the scanning plane, and similar results obtained by selecting circular polarization or light polarized parallel to the scan plane, indicated that transport distances in the plane of the sample were invariably shorter than $\lambda/2$. Under these conditions, despite negligible absorption (l_α is more than four orders of magnitude larger than l^*), electromagnetic energy is severely attenuated in less than a single spatial period. This implies that the light field emitted by dopant ions within our samples does not propagate or diffuse at all, but assumes a distribution similar to that of a three-dimensional evanescent field as the result of lossless reflection between particles. The short- l^* values deduced from our CBS measurements set an upper limit on coherence lengths that is somewhat less than a wavelength. This has very important implications [39] that should manifest themselves in other ways that we describe next.

When transport distances are shorter than the spatial scale necessary for interference, namely half a wavelength, the optical “coherence” length l_c is limited to a subwavelength value ($l_c \leq l^* < \lambda/2$). Such a short l_c precludes completely coherent scattering, apart from that produced by coherent light that never enters the medium but scatters from the surface itself. Hence the intensity fluctuations usually referred to as speckle [40] in the scattered light field of a coherent source should be greatly reduced. Experimentally, we found that indeed linearly polarized laser light scattered in the backward direction from our samples exhibited only $\pm 30\%$ intensity fluctuation during slow angular scans through the central range. For coherent input and stationary scatterers, this modulation is normally 100%, since all scattered light contributions are phase-coherent for a fixed configuration [29]. Time-averaging by sample motion is customarily necessary to extract meaningful field correlation functions. As expected, the residual noise in our experiment dropped from $\pm 30\%$ to $\pm 2\%$ when the sample was rotated about the beam axis at 2 rpm, confirming its origin as coherent speckle. However, the relatively small intensity fluctuations in back-scattered light made it possible to observe CBS cones without spinning the sample at all.

From the angular interval of 0.63 mrad between peaks and valleys in CBS scans of stationary samples, we inferred a limiting coherence “aperture” for the system of $d = 2\lambda/\Delta\theta = 2.0$ mm. This was in excellent agreement with the ~ 2 -mm diameter of the incident beam used to make the measurements, indicating that the speckle derived from reflective particles at the sample surface separated by less than the beam diameter, rather than from multiple scattering in the powder interior. Very much coarser speckle deriving from multiply scattered light with extremely short l^* was absent in CBS scans over angular ranges of up to 600 mrad when the sample was not rotationally averaged. This set a limit on the coherence length of $l_c < 1.3 \mu\text{m}$, independently of but in good accord with our CBS measurements.

Wide-angle photographs were also taken of electron-excited spots as small as 1 mm^2 , to check for evidence of

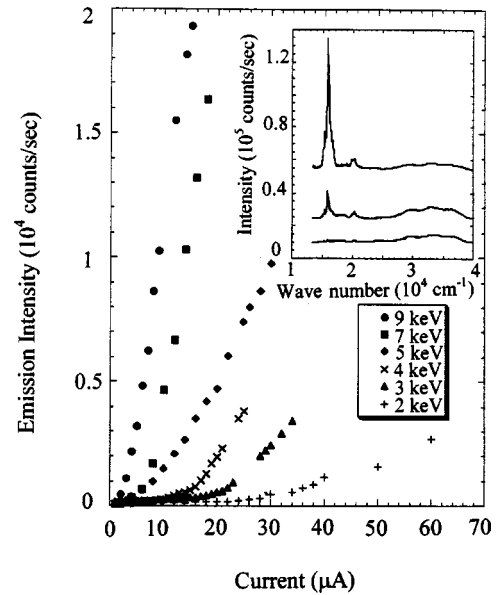


FIG. 5. Emission intensity vs current at $\lambda_{em} = 633$ nm in Pr: δ - Al_2O_3 nanoparticles, and electron energy (1–10 keV). Inset: emission spectra of Pr: δ - Al_2O_3 illustrating growth of the red transition with increasing current at 7 keV.

speckle in *emission*. A lensless Polaroid Land Film cassette was used outside the vacuum chamber for this purpose. No evidence was found for intensity fluctuations greater than 10% throughout solid angles as large as 0.04 sr, limited by chamber window size. The observation of uniform intensity over such a wide angular range eliminated the possibility of light emission in any given direction arising from coherent laser source regions in the powder with effective cavity lengths greater than the wavelength. We are led to conclude that above threshold, light from our samples is either generated in a fundamentally incoherent manner or it derives from an incoherent assembly of coherent sources that is indistinguishable from an incoherent source.

The ratio of the “coherent” peak intensity to the “incoherent” background was consistently less than 1.9 in numerous CBS experiments performed with different samples. Low ratios were observed with linear polarizations parallel/perpendicular to the scanning plane, and with circular polarization in the helicity-preserving channel. This is very much lower than the theoretical value of 2, characteristic of the diffusive regime [17], but may be due to experimental limitations. Experiments are underway with a new CBS apparatus to check whether low contrast in our samples is due to stray light contributions to the background or to recurrent scattering.

Additional perspective is provided by results for luminescence in Pr: δ - Al_2O_3 powder excited at various electron energies. Red emission from Pr^{3+} exhibits thresholds (Fig. 5) like that of ultraviolet emission in Ce^{3+} : δ - Al_2O_3 . Changes in slope at threshold are abrupt at low energies. They shift to lower currents and become less distinct as electron energy increases. Output curves also steepen at higher energies. These trends can be explained semiquantitatively by calculating electron penetration in Al_2O_3 versus energy using the

Monte Carlo code CASINO [41]. In the range 1–3 keV, the average penetration depth was less than the mean transport distance l^* , making it less than the length scale over which radiative transport is effective. Hence *significant radiant loss* from the excitation volume through the vacuum interface is possible in this energy range. On this basis, it is understandable that observed thresholds were strongly voltage-dependent between 1 and 3 keV, being highest for the lowest voltage. At a *fixed current* of 20 μA , the voltage threshold for laser action was reached experimentally in the neighborhood of 4–5 keV. The calculated penetration depth at this threshold voltage was comparable to the measured l^* . Under these conditions, energy is deposited efficiently within a volume $(\sim l^*)^3$, from which comparatively little radiant loss is possible through the vacuum interface. Over 4 keV, the optical output curves developed more curvature, as expected for amplification without feedback from a source lying deeper within the inverted medium [33].

The inset of Fig. 5 contains raw spectral emission data from the Pr sample. The separation of dominant features at 15 810 and 16 000 cm^{-1} is the same as that of the two dominant spectroscopic sites in Pr: β'' - Al_2O_3 , so these lines may be assignable either to the ${}^3P_0 \rightarrow {}^3H_6$ (4964 cm^{-1} π) and ${}^3P_0 \rightarrow {}^3H_6$ (4769 cm^{-1} σ) transitions of Pr^{3+} , respectively, or to one of these transitions at two different sites [42]. Since neither red transition quenches strongly as current is increased, we favor an assignment to one of these transitions at the two distinct sites. Most other features in the blue-red spectral region arise from 3P_0 , 3P_1 , and 3P_2 emissions, transitions from 1I_6 and 1D_2 being spin-forbidden. The three weak, ultraviolet bands are tentatively assigned to 1S_0 decays terminating on the 3P , 1D , and 1G levels [43].

V. CONCLUSIONS

The observations of spectral quenching behavior (Fig. 2), emission thresholding, and linear output above threshold [Figs. 3(a) and 5] collectively furnish compelling evidence of Ce^{3+} and Pr^{3+} laser action in the 1–4-keV range. Since conventional cavities support continuous laser action only with high reflectivity mirrors, these observations imply that light experiences nearly total reflection in three dimensions within our samples, in agreement with CBS measurements showing directly that scattering is so severe that light propagates forward less than half a wavelength irrespective of direction or polarization. Given that we find $l_c < l^* < \lambda$ in the absence of significant absorption ($\lambda \ll l_\alpha$), these experimental results suggest that light generated by an impurity ion within our powders acquires a spatial distribution that resembles that of a 3D evanescent wave [39]. Lacking any other consistent explanation, we conclude this behavior results from strong localization [10,11,44]. Emission is evidently stimulated co-

herently over distance scales of tens of nanometers in our samples, but spatial randomization on length scales of half a wavelength or more precludes directionality or mode selectivity. Backscattered light (and laser output) appears to be virtually speckle-free, consistent with its subwavelength effective coherence length. Finally, all frequencies within the luminescent linewidth experience comparable gain and feedback independent of observation angle, just as expected for continuous, truly “random” laser action.

Numerous applications for laser phosphors can be imagined in conventional lighting and displays. Though the brightness of existing phosphors in televisions, fluorescent lights, plasma, and field emission displays is strictly limited by the spontaneous-emission rate, this limitation can be overcome with stimulated emission. The absence of speckle could also facilitate large-area, submicron optical lithography. However, while doped, dielectric nanophosphors may provide a versatile family of emissive materials for novel light sources, many fundamental advances can be expected to emerge from these findings. Confinement of light within subwavelength regions may mediate new or enhanced nonlinear phenomena associated with ultraslow light, recurrent scattering, and surface resonances. Omnidirectional stimulated emission will be achievable on new transitions, in new wavelength ranges, with excitation methods not previously feasible in dielectrics. This prospect is illustrated by our own results for Ce^{3+} , which are the first to demonstrate continuous laser action on its ultraviolet transition by any means. Studies of pseudogap filtering, optical coherence, and speckle in the proximity of the localization “edge” should now be feasible in nanodielectrics. Unlike electrons, photons do not interact with one another at low energies in vacuum. Consequently, research on these topics will furnish perspectives to complement existing knowledge from electron studies of wave transport in a wide variety of disordered systems [45].

Note added in proof. Effective cavity size was also large in research on dye-doped silver colloids inside quartz resonators that have been reported to support continuous laser action [Phys. Rev. Lett. **82**, 4811 (1999)]. There, morphology-dependent resonances of a macroscopic cavity determined spectral modes of the output.

ACKNOWLEDGMENTS

The authors wish to thank K. L. Schepler, S. Lipson, E. Leith, and G. W. Ford for useful discussions, and J. M. Glowonia and B. Furman for assistance with backscattering measurements. We gratefully acknowledge research grants from the National Science Foundation (DMR-9975542), the Army Research Office (DAAD19-99-1-0229), and U.S. DOD–Air Force (F49620-99-1-0158).

[1] M. P. Van Albada and A. Lagendijk, Phys. Rev. Lett. **55**, 2692 (1985).

[2] V. M. Markushev, V. F. Zolin, and Ch. M. Briskina, Sov. J.

Quantum Electron. **16**, 281 (1986).

[3] A. Z. Genack and N. Garcia, Phys. Rev. Lett. **66**, 2064 (1991).

[4] J. X. Zhu, D. J. Pine, and D. A. Weitz, Phys. Rev. A **44**, 3948

- (1991); T. M. Nieuwenhuisen and J. M. Luck, *Phys. Rev. B* **48**, 569 (1993).
- [5] C. Gouedard, D. Husson, C. Sauteret, F. Auzel, and A. Migus, *J. Opt. Soc. Am. B* **10**, 2358 (1993).
- [6] N. M. Lawandy, R. M. Balachandran, A. S. L. Gomes, and E. Sauvain, *Nature (London)* **368**, 436 (1994).
- [7] M. Siddique, R. R. Alfano, G. A. Berger, M. Kempe, and A. Z. Genack, *Opt. Lett.* **21**, 450 (1996).
- [8] M. A. Noginov, N. E. Noginov, H. J. Caulfield, P. Venkateswarlu, T. Thompson, M. Mahdi, and V. Ostroumov, *J. Opt. Soc. Am. B* **13**, 2024 (1996).
- [9] D. Wiersma and A. Lagendijk, *Phys. World* **10** (1), 33 (1997).
- [10] S. John, *Phys. Rev. Lett.* **53**, 2169 (1984); S. John, *Phys. Today* **44** (5), 32 (1991).
- [11] P. W. Anderson, *Philos. Mag. B* **52**, 505 (1985).
- [12] V. S. Letokhov, *Sov. Phys. JETP* **26**, 835 (1968).
- [13] S. John and G. Pang, *Phys. Rev. A* **54**, 3642 (1996).
- [14] R. M. Balachandran, N. M. Lawandy, and J. A. Moon, *Opt. Lett.* **22**, 319 (1997).
- [15] D. Wiersma and A. Lagendijk, *Phys. Rev. E* **54**, 4256 (1996).
- [16] G. A. Berger, M. Kempe, and A. Z. Genack, *Phys. Rev. E* **56**, 6118 (1997).
- [17] D. S. Wiersma, M. P. van Albada, B. A. van Tiggelen, and A. Lagendijk, *Phys. Rev. Lett.* **74**, 4193 (1995).
- [18] D. S. Wiersma, P. Bartolini, A. Lagendijk, and R. Rhigini, *Nature (London)* **390**, 671 (1997).
- [19] M. Kaveh, M. Rosenbluh, and I. Freund, *Nature (London)* **326**, 778 (1987).
- [20] G. Gbur and E. Wolf, *Opt. Lett.* **24**, 10 (1999); E. Wolf, T. Shirai, G. Agarwal, and L. Mandel, *ibid.* **24**, 367 (1999).
- [21] E. Leith, C. Chen, H. Chen, Y. Chen, D. Dilworth, J. Lopez, J. Rudd, P.-C. Sun, J. Valdmanis, and G. Vossler, *J. Opt. Soc. Am. A* **9**, 1148 (1992).
- [22] P. Siqueira and K. Sarabandi, *IEEE Trans. Antennas Propag.* **48**, 317 (2000); K. Sarabandi and P. R. Siqueira, *ibid.* **45**, 858 (1997).
- [23] R. C. Polson, A. Chipouline, and Z. V. Vardeny, *Adv. Mater.* **13**, 60 (2001).
- [24] H. Cao, Y. G. Zhao, S. T. Ho, E. W. Seelig, Q. H. Wang, and R. P. H. Chang, *Phys. Rev. Lett.* **82**, 2278 (1999); H. Cao, Y. Ling, J. Y. Xu, C. Q. Cao, and P. Kumar, *ibid.* **86**, 4524 (2001).
- [25] R. K. Thareja and A. Mitra, *Appl. Phys. B: Lasers Opt.* **71**, 181 (2000).
- [26] A. C. Sutorik, S. S. Neo, T. Hinklin, R. Baranwal, D. R. Treadwell, R. Narayanan, and R. M. Laine, *J. Am. Ceram. Soc.* **81**, 1477 (1998); R. M. Laine, K. Waldner, C. Bickmore, and D. Treadwell, U.S. Patent, 5,614,596 (March 1997).
- [27] S. Brunauer, P. H. Emmett, and E. Teller, *J. Am. Chem. Soc.* **60**, 309 (1938).
- [28] Y. Kuga and A. Ishimura, *J. Opt. Soc. Am. A* **1**, 831 (1984).
- [29] P. E. Wolf and G. Maret, *Phys. Rev. Lett.* **56**, 1471 (1986).
- [30] S. Okamoto, K. Kato, and T. Arakawa, *J. Alloys Compd.* **192**, 37 (1993).
- [31] D. J. Ehrlich, P. F. Moulton, and R. M. Osgood, Jr., *Opt. Lett.* **4**, 184 (1979).
- [32] C. D. Marshall, J. A. Speth, S. A. Payne, W. F. Krupke, G. J. Quarles, V. Castillo, and B. H. T. Chai, *J. Opt. Soc. Am. B* **11**, 2054 (1994); N. Sarukura, M. A. Dubinskii, Z. Liu, V. V. Semashko, A. K. Naumov, S. L. Korableva, R. Y. Abdulsabirov, K. Edamatsu, Y. Suzuki, T. Itoh, and Y. Segawa, *IEEE J. Sel. Top. Quantum Electron.* **1**, 792 (1995).
- [33] R. V. Ambartsumyan, N. G. Basov, P. G. Kryukov, and V. S. Letokhov, *Prog. Quantum Electron.* **1**, 109 (1970).
- [34] R. M. Balachandran and N. M. Lawandy, *Opt. Lett.* **20**, 1271 (1995).
- [35] E. Akkermans, P. E. Wolf, R. Maynard, and G. Maret, *J. Phys. (France)* **49**, 77 (1988).
- [36] E. Akkermans, P. E. Wolf, and R. Maynard, *Phys. Rev. Lett.* **56**, 1471 (1986).
- [37] L. G. DeShazer, S. C. Rand, and B. A. Wechsler, *Laser Crystals*, in *Handbook of Laser Science and Technology*, edited by M. J. Weber (CRC, Boca Raton, FL, 1987), Optical Materials Vol. 5, Pt. 3, pp. 281–338.
- [38] M. Born and E. Wolf, *Principles of Optics*, 4th ed. (Pergamon, New York, 1970), p. 633.
- [39] J. W. Goodman, *Statistical Optics* (Wiley, New York, 1985), p. 206.
- [40] J. C. Dainty, *Laser Speckle and Related Phenomena* (Springer, New York, 1984).
- [41] P. Hovington, D. Drouin, and R. Gauvin, *Scanning* **19**, 1 (1997).
- [42] Phyllis Nelson, Ph.D. dissertation, University of California, Los Angeles, 1995. Nd site splitting assumed [A_{20} comparable: B. Dunn *et al.*, *J. Solid State Chem.* **73**, 235 (1988)].
- [43] L.-S. Lee, S. C. Rand, and A. L. Schawlow, *Phys. Rev. B* **29**, 6901 (1984).
- [44] A. F. Ioffe and A. R. Regel, *Prog. Semicond.* **4**, 237 (1960).
- [45] P. A. Lee and T. V. Ramakrishnan, *Rev. Mod. Phys.* **57**, 287 (1985).